Volume 24, No 4 | International Journal of Radiation Research, October 2026

Experimental forensic aspects of ionizing radiation: A postmortem study on supra-lethal dose irradiated rats

W.T. Tawfik[1], Z.S. Said[2], M.R. Mohammed[3], M.M. Ahmed[3*], S.A. Montaser[3]

[1]*Forensic Medicine and Clinical Toxicology Department, Faculty of Medicine, Ain Shams University, Egypt*
[2]*Radiation Safety Department, Nuclear and Radiation Safety Research Centre, Egyptian Atomic Energy Authority, Cairo, Egypt*
[3]*Radiation Biology Department, National Centre for Radiation Research and Technology (NCRRT), Egypt, Egyptian Atomic Energy Authority, Nasr City, Egypt*

► ***Original article***

Corresponding author:
Mahmoud M. Ahmed, Ph.D.,
E-mail:
mahmoud_70mohameds@yahoo.com

Received: February 2025
Final revised: March 2026
Accepted: March 2026

Int. J. Radiat. Res., October 2026; 24(4): 1133-1141

DOI: 10.61186/ijrr.24.4.26

Keywords: *Supra-lethal dose radiation, postmortem changes, cytogenetic analysis, biochemical estimation, liver and brain histopathology.*

ABSTRACT

Background: Forensic science rarely deals with radiation accidents and radiotherapy doses, which may lead to death in the scientific and medical fields. These are the consequences and causes of death because of supra-lethal dose (20 Gy) of radiation exposure and detecting the times of death and monitoring the postmortem changes in the different groups. ***Materials and Methods:*** The experiment was designed using four groups of Sprague-Dawley albino rats (6 male rats each). Rats were exposed to supra-lethal (20 Gy) with a dose rate (0.717 KGy/h) gamma radiation (Cobalt-60 γ-radiation).The postmortem study was conducted in four time intervals (0, 6, 8 and 20 hours). Comparison was done for verification of the two goals. The first one is to monitor the incidence of death and the second is to investigate the postmortem changes over time between groups. The study included cytogenetics, biochemical and histopathology analysis. ***Results:*** showed a non-traditional interpretation of death resulting from supra-lethal dose radiation exposure. Moreover, the study scrutinized death timing via the different groups and presenting a comparison between the physiological changes that occurred over time. ***Conclusion:*** The main unique causes of death after supra-lethal dose irradiation are devastation of the bone marrow and collapse of its vital function, microbiome invasion, andloss of communication pathways between cells and each other and between cells and organs, then a multi-organ succession failure.

INTRODUCTION

Acute exposure to high doses of ionizing radiation, particularly supra-lethal levels, produces distinctive clinical and pathological effects that are often unfamiliar to many physicians and specialists in both scientific and medical fields. Acute Radiation Syndrome (ARS) can rapidly progress to death, yet awareness of its specific manifestations and associated health risks remains limited. In response, international health organizations have developed educational programs, diagnostic guidelines, and specialized emergency units to improve preparedness and management of radiation injuries, encompassing a variety of incident types, from accidents to occupational exposures [1]. Within forensic medicine, there is a notable scarcity of clear, evidence-based information on determining the cause of death due to high-dose radiation exposure, as well as practical methodologies for distinguishing such cases from other causes. Determining the postmortem interval is a central task in forensic investigations, providing critical insight into the timing and circumstances of death, which in turn assists in reconstructing events in suspicious or complex cases [2].

Postmortem changes are influenced by a range of environmental and intrinsic factors. External variables such as air humidity, temperature, and animal or insect activity can alter decomposition processes [3], while internal factors including age, sex, and physiological or pathological status complicate postmortem interval estimation [4]. Moreover, gene expression alterations can occur after death, as certain genes become more active postmortem, potentially serving as novel forensic indicators [5]. Conventional postmortem interval estimation techniques - physical, biochemical, and entomological - are often limited by environmental variability, necessitating exploration of alternative methods such as cytogenetic and physicochemical analyses [6]. Thanatochemistry, or postmortem chemistry, offers quantitative markers for postmortem interval estimation, though the selection of optimal parameters and tissue types remains a challenge [7]. Physical and biochemical changes begin immediately after death and progress until complete tissue disintegration [8]. For instance, increased nitric oxide levels have been observed in postmortem brain tissue under oxidative stress [9, 10], and the

[Downloaded from mail.ijrr.com on 2026-11-11]

[DOI: 10.61186/ijrr.24.4.26]

concentrations of nitrogenous metabolites such as ammonia, hypoxanthine, and uric acid can vary over time, reflecting protein catabolism and purine metabolism [11, 12].

Acetylcholinesterase (AChE) and plasma cholinesterase (ChE) are key enzymes in neural and systemic physiology, with AChE found in the nervous system and erythrocyte membranes, and ChE in plasma, liver, cerebrospinal fluid, and glial cells [13,14]. Their postmortem activity changes may provide useful forensic markers. Given that conventional postmortem interval estimation techniques are affected by numerous confounding factors, integrating biochemical and cytogenetic methods with histopathological evaluation may offer more reliable and specific results. Therefore, this is one of the pioneer experimental forensic studies to integrate cytogenetic, biochemical, and histopathological analyses to determine mechanism and time of death following supra-lethal γ-irradiation in rats.

The present work aims to follow the gained findings at the different postmortem intervals to interpret and detect mechanism of death via a supra-lethal dose of irradiation.

MATERIAL AND METHODS

Experimental animals and irradiation

Twenty four Male Sprague-Dawley Albino rats weighing 240-250 gm (10-12 weeks old) were acquired from the animal house of the National Centre for Radiation Research and Technology (NCRRT). They were accommodated in polypropylene cages for food and water ad libitum, regarding typical laboratory circumstances and regulated temperature 22 ± 2°C, 50–60% humidity, 12 h light/dark cycle, throughout the experiment. Rats were exposed to supra-lethal (20 Gy) with dose rate (0.717 KGy/h) gamma radiation at the National Centre for Radiation Research and Technology (NCRRT), Atomic Energy Authority, Cairo, Egypt, using a Cobalt 60 unit, with whole shielding for the working staff.

Ethical considerations

Animal welfare is paramount. Researchers minimized pain and suffering and followed the ethical guidelines for animal research in accordance to the rules of the experimental research ethics approved bythe Ethics Committee at the NCRRT, which belongs to the Egyptian Atomic Energy Authority (Certificate No.: F/38A/22). The minimum number of animals estimated to provide valid results was used.

Experimental design and groups

Twenty-four male Sprague-Dawley albino rats were divided into 4 equal groups (n=6). Animals were left until death (Preliminary observation to determine the approximate time of death after irradiation). After irradiation, rats were divided into four equal groups (n = 6) according to the postmortem interval: Group I (0 h), Group II (6 h), Group III (8 h), and Group IV (20 h).

Tissue preparation

After animal dissection, the brain and liver tissues were perfused with a phosphate-buffered saline (PBS) solution, pH 7.4, containing 0.16 mg/ml heparin to remove any red blood cells and clots. Then, tissues were frozen at −20°C until biochemical analysis. One gram of tissue was homogenized in 5-10 ml cold buffer (i.e. 50 mM potassium phosphate, pH 7.5), centrifuged at 4000 r.p.m for 15 minutes under cooling conditions, the supernatant was assayed immediately according to each kit instructions. Liver and brain tissues were homogenized with PBS (0.5 gm tissue in 5 ml PBS) for biochemical investigations.

Cytogenetic study

Micronucleus test (Micronucleus Cytome Assay): Bone marrow samples were collected from the rat's femur at the sacrificing time, according to Schmid [15] with modification for bone marrow assessment according to Findly and Satish *et al.* (with detail will be mentioned in discussion section), three-sample slides were prepared for each animal for the micronucleus assay. The slides were stained with 5% Giemsa stain diluted in phosphate buffer (Na_2HPO_4 0.06 M and $KH_2PO_4$0.06 M, pH 6.8) [16].

Biochemical parameters

Homogenization

Liver tissue is typically homogenized in a buffer (e.g., phosphate buffer, PBS) to smash down the cells and liberate their contents. The buffer often includes a detergent (like Triton X-100 or SDS) to help solubilize proteins and other cellular components.

Determination of AChE level (brain homogenate)

Using Acetylcholinestrase Activity Colorimetric Assay Kit for tissue purchased from Abcam with catalog number ab287842 (UK). The method depending on formation of colored intermediated from converting acetylcholine to coline. The color represents the concentration of enzyme. The colored products measured at (OD 570 nm).

Determination of nitric oxide (NO) (liver homogenate)

NO was measured according to the manufacturer instruction using the QuantiChrom TM Nitric Oxide Assay Kit (D2NO-100) USA. This BioAssay Systems' Assay Kit was designed to accurately measure NO production following reduction of nitrate to nitrite with improved Griess method. The absorbance was read at

[Downloaded from mail.ijrr.com on 2026-11-11]

[DOI: 10.61186/ijrr.24.4.26]

540 nm.

Determination of uric acid (liver homogenate)

Liver homogenate uric acid was determined using BioMed-Uric acid L.S. purchased from Egypt. Uric Acid is oxidized by Uricase to allantoin and hydrogen peroxide. The released hydrogen peroxide together with DCHBS* and 4-aminoantipyrine, in the presence of peroxidase, forms a red dye compound. The intensity of the red color produced is directly proportional to the uric acid quantity. Color was measured at wave length of 500-550 nm.

Determination of urea (liver homogenate)

Urea is the major product of protein and nitrogen metabolism and protein catabolism. Series of reaction involved in the assay starts as urea hydrolyzed in the presence of water and urease to produce ammonia and carbon dioxide. In the presence of glutamate dehydrogenase and reduced nicotinamide adenine dinucleotide (NADH), the ammonia combines α-ketoglutarate to produce L-glutamate. The rate decrease in the NADH concentration is directly proportional to the urea concentration in the specimen. It is determined by measuring the absorbance at 340 nm.

Urea level in liver homogenate was estimated using BioMed diagnostic Urea/BUN-(UV) enzymatic method. It purchased from Egypt with reference number URF220050.

Histopathological studies

Autopsy samples were taken from the liver & brain of rats in different groups and fixed in 10% formol saline for twenty-four hours. Washing was done in tap water, then serialdilutions of alcohol (methyl, ethyl, and absolute ethyl) were used for dehydration. Specimens were cleared in xylene and embedded in paraffin at 56 degrees in a hot air oven for twenty-four hours. Paraffin beeswax tissue blocks were preparedfor sectioning at 4-microns thickness by a rotary LEITZ microtome. The obtained tissue sections were collected on glass slides, deparaffinized, and stained with hematoxylin & eosin stain [17], for examination through the light microscope.

Statistical analysis

The data were expressed as mean ± standard error (SE). Statistical analysis was performed using the Statistical Package for the Social Sciences (IBM SPSS version 20). One-way analysis of variance (ANOVA) was applied, followed by Tukey multiple comparison tests. *P*-values < 0.05 were considered significant [18].

RESULTS

Table 1 reviews the postmortem events at 0, 6, 8, and 20 hrs in the bone marrow using the micronucleus test cytome assay. The results reflect the direct impact of exposure to high levels of radiation, leading to death. A significant decline in normal myeloblast cells was observed compared to erythrocytes, until disappearing completely after 20 hrs. Additionally, a clear and significant increase in the morphological abnormalities was noted in erythrocytes and myeloblast cells.

Table 1. Quantitative micronucleus cytome assay of rat bone marrow cells at different postmortem intervals (0, 6, 8, and 20 h) following high-dose radiation exposure. Data show mean ± standard error (SE) counts for various cell types, including erythrocytes (normal, abnormal morphology, micronucleated), myeloblasts (normal, abnormal morphology, micronucleated), apoptotic, necrotic, megakaryocytes, mast cells, stromal reticular cells, and adipocytes.

Cell Types		Postmortem Time Intervals (Mean±SE)			
		Zero Time Group	6h. Postmortem Group	8h. Postmortem Group	20h postmortem Group
Erythrocytes	Normal Erythrocytes	57.72±0.47	a 37.67±0.36	ab 41.22±0.66	abc 15.99±0.53
	Abnormal Morphology	12.03±0.15	a 16.8±0.18	ab 18.46±0.56	abc 64.68±0.43
	Micronucleated	4.3±0.11	a 6.03±0.16	b 4.14±0.20	abc 0
Myeloblasts	Normal Myeloblast	2.06±0.09	2.25±0.13	2.5±0.08	abc 3.86±0.18
	Abnormal Morphology	2.42±0.10	a 4.73±0.19	ab 3.03±0.13	abc 0.64±0.08
	Micronucleated	1.43±0.12	a 2.62±0.12	b 1.45±0.06	abc 0
Apoptic		6.2±0.10	a 1.45±0.13	ab 0.72±0.12	abc 2.24±0.21
Necrotic		2.33±0.10	a 3.35±0.17	ab 9.98±0.16	abc 10.42±0.25
Megakaryocytes		0	a 2.07±0.2	ab 1.34±0.05	abc 0.51±0.12
Mast Cells		1.17±0.08	a 3.47±0.10	ab 3.77±0.04	abc 0
Stromal Reticular Cells		0	a 4.7±0.16	ab 2.67±0.09	bc 0.26±0.08
Adipocytes		6.53±0.2	a 14.87±0.10	10.74±0.28	abc 1.41±0.15

Statistical differences are indicated by superscript letters, where: a: significant as compared with the zero-time group. b: significant as compared with the 6 hours postmortem group. c: significant as compared with the 8 hours postmortem group.

The micronucleated erythrocytes and myeloblast cells increased at 0 and 6 hrs, followed by a decrease after 8 hrs and complete disappearance in the 20-hr group. Whereas, the results indicated a gradual significant decrease in apoptic cells of erythrocytes (exceptthe 8-hr group) and myeloid cells, accompanied by a gradual significant increase in necrotic cells (figure 1).

The results reported a fluctuation of megakaryocytes, mast cells, stromal reticular cells, and adipocyte counts in certain groups. Where it recorded a significant increase of megakaryocytes

[Downloaded from mail.ijrr.com on 2026-11-11]

[DOI: 10.61186/ijrr.24.4.26]

and stromal reticular cells in the 6-hr group, then a gradual decrease through the next time intervals. On the other hand, Mast cells showed a significant increase from 0 time up to 8 hrs, then suddenly vanished at 20 hrs. Finally, adipocytes showed a significant increase from 0 time to 6 hrs interval, then a significant decrease in the following time intervals.

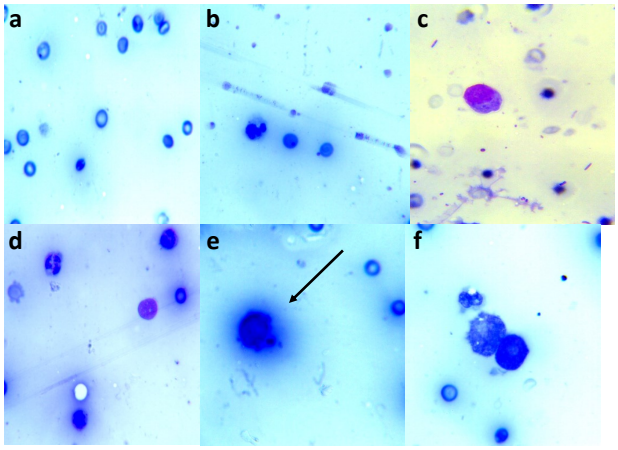


Figure 1. Representative photomicrographs of bone marrow cells evaluated in the micronucleus (MN) cytome assay at different postmortem intervals. **(a)** Normal erythrocyte; **(b)** micronucleated erythrocytes; **(c)** normal myelocyte; **(d)** apoptotic cells **(e)** micronucleated myelocytes; **(f)** necrotic cells. (Magnification 1000X).

Table 2 evaluated some indicated biochemical investigations in rats' brain and liver homogenate tissues for postmortem intervals at 0, 6, 8, and 20 hrs. Results recorded the maximum significant increase in all measured parameters at 20 hrs postmortem. The values of acetylcholine esterase in the brain and nitric oxide, uric acid and urea in the liver were increased gradually from zero to 20 hrs interval, except nitric oxide and urea at 8 hrs interval fluctuated.

Table 2. Biochemical markers in brain and liver homogenates of rats at different postmortem intervals (0, 6, 8, and 20 h) following radiation exposure. Parameters measured include brain acetylcholine esterase (AChE, nmol/g protein) and liver nitric oxide (NO, pmol/mg), uric acid (UA, U/mg), and urea (U/mg). Data are expressed as mean ± SE.

Groups	Brain Homogenate	Liver Homogenate		
	Acetylcholine Esterase (nmol/g/protein)	Nitric Oxide (pmol/mg)	Uric Acid (U/mg)	Urea (U/mg)
Zero Time	1.05±0.03	22.87± 0.98	1.55± 0.088	41.83± 0.6
6 hours postmortem	1.12±0.023	24.6± 1.49	1.83± 0.09	48.67± 2.82^{a}
8 hours postmortem	2.65±0.042^{ab}	22.22± 0.62	3.21± 0.095^{ab}	40.63± 3.0^{b}
20 hours postmortem	5.15±0.05^{abc}	25.43± 0.6^{C}	5.9± 0.11^{abc}	61.83± 1.2^{abc}

Statistical differences are indicated by superscript letters, where: a: significant when compared withthe zero-time group. b: significant when compared with the 6 hours postmortem group. c: significant when compared with the 8 hours postmortem group. Nmol: nanomole. g: gram. pmol: picomole u\mg: unit per microgram

Histopathological findings

Observation of changes in rat liver and brain samples at different postmortem intervals with Hematoxylin and eosin (HE) staining. From a postmortem interval of 0 h to that of 20 h, the severity of rat liver cell autolysis continuously increased, as shown in the micrographs of postmortem liver (20X magnification).

Liver histopathology

As shown in figure 2 at 0 h, all of the liver cells and cell nuclei were clearly visible. At 6 hours after death, the nucleiwere observed to shrink, and partial degradation was seen in the hepatocytes. After 8 hours, the nucleicompletely disappeared, and 20 hours after death, the liver cell structure itself had mostly disappeared.

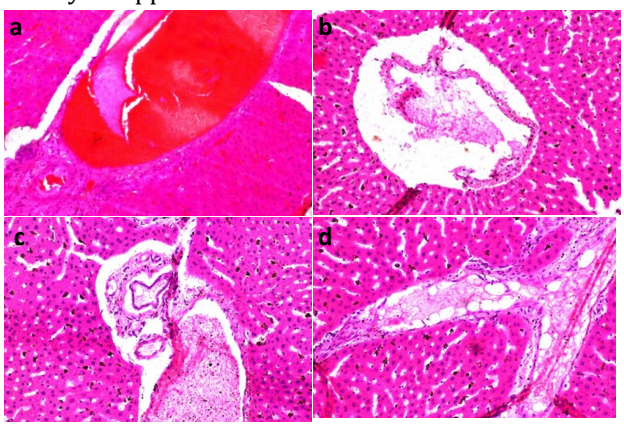


Figure 2. Histopathological changes in rat liver tissue at different postmortem intervals after radiation exposure. Hematoxylin and eosin (H&E) staining, magnification 20X. **(a)** 0 h: normal hepatic architecture with intact nuclei; **(b)** 6 h: nuclear shrinkage and partial hepatocyte degradation; **(c)** 8 h: complete nuclear disappearance; **(d)** 20 h: extensive autolysis and loss of cellular structure. Additional pathological changes include severe central vein dilatation and congestion, hemolysis in the central zone, portal vein congestion with connective tissue hyalinization, hepatocyte nuclear pyknosis, bile duct epithelial changes, endothelial sloughing, vascular fibrillation, bile duct shrinkage, diffuse hemosiderosis, and vacuolization in portal structures.

Severe dilatation and congestion of the central vein associated with hemolysis of the blood component of the central zone of the vein figure 2. The portal area showed severe congestion in the portal vein, with hyalinization of the portal connective tissue as well as nuclear pyknosis of the hepatocytes and epithelium of the bile ducts.

There was sloughing in the endothelium cells lining the central vein with fibrillation of the vascular component. The portal area showed shrinkage of the bile ducts associated with fibrillation of the vascular component as well as diffuse hemosiderosis between the hepatocytes. There was vacuolization in the component of the portal area.

[Downloaded from mail.ijrr.com on 2026-11-11]

[DOI: 10.61186/ijrr.24.4.26]

Brain histopathology

The striatum of the cerebrum as well as the cerebellum showed severe congestion in the blood vessels and capillaries associated with diffuse gliosis figure 3.

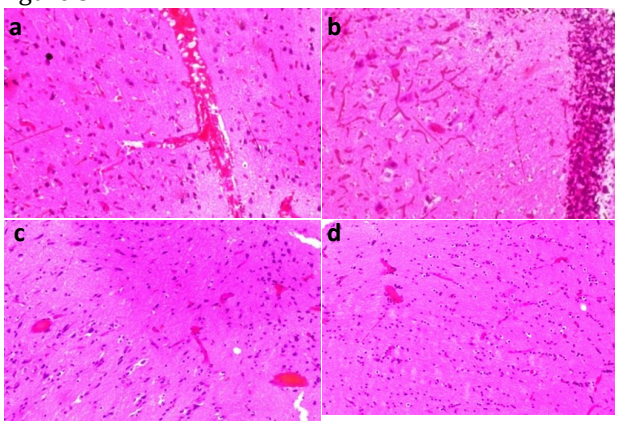


Figure 3. Histopathological changes in rat brain tissue at different postmortem intervals after radiation exposure. Hematoxylin and eosin (H&E) staining, magnification 20X. **(a)** 0 h: normal brain architecture; **(b)** 6 h: severe vascular and capillary congestion; **(c)** 8 h: increased gliosis and tissue degeneration; **(d)** 20 h: pronounced congestion with diffuse gliosis in the striatum of the cerebrum and cerebellum.

DISCUSSION

A series of biochemical and pathological processes happen after death, resulting in considerable changes in the structure and composition of the body. Because many of these changes occur sequentially, evaluation of the types and degrees of changes may help in estimation of time of death [19]. Postmortem interval estimation requires the calculation of data, which changes constantly and proportionally from the time of death with a linear process along a time-dependent curve [20]. Furthermore, the cause of death is a main part of forensic pathology, which needs a meticulous process involving systematic autopsy, subsequent morphological examination, toxicological analysis, and others [21].

Forensic medical analysis is a challenging tool to establish the details of any accident. Radiation experts can help formulate the possible scenarios and determine further investigative leads [22], after exposure to different types and sources of ionizing radiation such as accidents in Hiroshima or Chernobyl, occupational catastrophes, severe radiotherapy with high doses or even heavy exposure as in disasters investigations. There are several studies investigated the ionizing irradiation's harmful actions, the most reliable and remarkable analyses are bone marrow and reduction of blood perfusion, chromosomal and cellular damages, and deleterious biochemical measurements [23].

Therefore, the present outcomes reviewed the postmortem events at 0, 6, 8, and 20 hrs via cytogenetic, biochemical and histopathological studies resulting from supra-lethal dose exposure (20 Gy). The cytogenetic analysis findings in the bone marrow cells using the micronucleus cytome assay reflects the direct impact of exposure to high levels of radiation leading to death.

There is a gradual depletion of myeloblasts in all groups, which was extensive in comparison to erythrocytes until it disappeared at 20 hrs that means severe impairment of the immunity, which can be attributed as the cause of death. On the other hand, there was an abnormal morphology of both erythrocytes and myeloblasts in all groups. The micronucleated erythrocytes and myeloblast cells increased at 0 and 6 hrs then decreased after 8 hrs and completely disappeared in the 20-hr group. There was a gradual significant decrease in apoptic cells of erythrocytes (except the 8-hr group) and myeloid cells, accompanied by a gradual significant increase in necrotic cells.

These findings may be discussed and interpreted according to the main known effect of radiation exposure that leads to depletion of the proliferation rate and mitotic index especially, at the 8 and 20 hrs intervals. This is accompanied by a decrease in the natural programmed cell death (apoptosis) of irradiated damaged cells and an increase in the necrosis rate from 0 to 20 hrs intervals. Stromal reticular cells were apparent in the 2 nd and 3rd groups which can be explained by the death of other types of cells so reticular cells became prominent as a backbone to bone marrow.

The nature of bone marrow is an integrated system that contains a multicellular pool (Structural, functional, and maintenance components). Science multipotent hematopoietic progenitors included in bone marrow that it considered the main immunological functional machinery. But also, there are other cells have additional functional, structural and maintenance roles as; megakaryocytes, mast cells, stromal reticular cells, and adipocytes [24]. Bone marrow stem cells can remain viable for several days after death. Studies show that some bone marrow stem cells, including hematopoietic stem cells and skeletal muscle stem cells, can survive for up to four days after death in mice. These cells can even retain their ability to differentiate into functional cells, such as muscle cells, and can be used in transplants. The current results reported that at zero-time megakaryocytes and stromal reticular cells were recorded zero and low count for mast and adipocytes but these frequencies from 6 to 20 hrs postmortem were gradually decreased. These fluctuation findings may be attributed to the diversity of each type of these cells to continue division after death [25].

Additionally, mast cells are part of the innate immune system. They are a normal cellular

[Downloaded from mail.ijrr.com on 2026-11-11]

[DOI: 10.61186/ijrr.24.4.26]

component of the bone marrow but are not very numerous in normal bone marrow. It represents immune effector cells, which play a major role in immunoglobulin responses. Ionizing radiation affects the functions of mast cells that are involved in radiation-induced tissue damage [26]. Whereas, adipocytes are also a major cell type within the bone marrow, filling excess space in the bone marrow cavity that accounts for up to 70% its volume. They play a dynamic role in systemic lipid metabolism, and provide a localized energy reservoir in the bone marrow [27]. So, after irradiation adipocytes represent a local energy source and support myeloid cell lineage regeneration in addition to maintaining progenitor differentiation capacity when systemic energy is limiting [28].

All mentioned cells exist in loose stroma made up of a wide meshwork of reticular cells which are a supporting element closely related to bone marrow hematopoiesis. Additionally, the bone marrow stroma contains cells with a stem-cell-like character that allows them to differentiate into bone, cartilage, adipocytes, and hematopoietic supporting tissues [29].

In comparison, with Sakr *et al.*, [30] bone marrow findings showed changes from 6 to 18 hours after death, described as gradual, progressive and regular. Cytoplasmic vacuolations and multilobulation of the nucleus of bone marrow cells appeared at 6 hrs postmortem. The appearance of budding and multilobulation of the nucleus at 10 hrs postmortem and some pyknotic nuclei and syncytium of the nucleus in 14 hrs postmortem, and 18 hrs postmortem showed loss of cellular details, absence of fat cells and necrosis of postmortem. In addition, Gururaj *et al.* [31] analysis reported that lysis in both the nuclear and cytoplasm was between 11 and 16 hrs postmortem. Complete loss of cellular morphology was observed at more than 16 hours postmortem.

On the other hand, present findings confirmed by Satish Babu *et al.* [32] who reported that no appreciable changes in the cellular morphology were detected in the bone marrow during the first 5 hrs after death. After this period, the autolytic changes were seen in the cells.

The presented results showed that normal erythrocytes were gradually decreased except at 8 hrs postmortem, but for morphological abnormalities were gradually declined from zero to 20 hrs postmortem. Findlay [33] reported the earliest change of erythroid nucleus lineage at the time of 1-2 hours postmortem, in the form of budding. By 2-3 hrs postmortem more pyknotic cells along with budding of nucleus was appreciated and by more than 3 hrs postmortem multilobulation of the nucleus was seen. Among granulocytes no change was appreciated in the time interval of 1-4 hrs postmortem. There was early myelocytes lysis by 7–8 hrs postmortem. Later by 8–12 hrs postmortem myelocytes lysis was observed in many of the cells. By more than 12 hrs postmortem appreciable myelocytes lysis was observed.

Kvacheva [34] reported that the period of time passed after radiation injury can be assessed on the basis of morphological characteristics of bone marrow. Under doses at which the hematopoietic form of radiation sickness takes place, the elements of stroma and plasma cells dominate in cellular composition. Later, after 4 weeks, granular lymphocytes appear. Then, morphological signs of early recovery can be observed: the number of hematopoietic stem cells and mitosis increase. Moreover, as stated by Suzuki *et al.* [35], the hematopoietic system stabilizes the number of all types of blood cells and immune homeostasis by the differentiation of the hematopoietic stem cells.

On the other hand, the concept of the postmortem biochemical analysis is one of the most dynamic supplementary measures for forensic pathologists, especially in cases where pathomorphological findings are poor, even if the clinical diagnostic criteria cannot be used due to agonal phenomena and/or postmortem interference [36].

Normally, AChE enzyme present in the nervous system and in the outer membrane of erythrocytes, while plasma ChE present in plasma, liver, cerebrospinal fluid and glial cells [14]. The principal function of AChE is to terminate neuronal transmission and signaling between synapses to prevent Ach distribution and activation of nearby receptors [36].

In the current study, huge significant elevation in AChE activities was recorded in (6, 8, and 20 hrs) postmortem brain tissue homogenates, reaching its maximum values (one-fold, 2.5 up to 5 folds) respectively when compared with the control group, revealing severe brain damage occurred after high-dose ionizing radiation exposure (20Gy). The brain tissue often showed stability when compared with other tissues, but in our study, death was due to high-dose irradiation, which aggressively affects the brain tissue AChE enzyme concentration and its effect prolongs even after death with a hallmark of high irradiation severity on the brain as stated by Krassner *et al.* [38]. Whereas, several experimental forensic studies focused on measuring cerebral AChE activity. The presented results coincide with Da Fonseca *et al.* [8] investigations that showed an increase in AChE activity in the brain at the time of 24 hrs when compared with the time of 0 hr.

Nitric oxide (NO) is produced in response to homeostatic, inflammatory, or mitogenic stimuli. It can produce hydroxyl radicals as well as nitrogen dioxide radicals [39]. In the present study, nitric oxide was evaluated in liver homogenate in different groups; it increased at 6 hrs and 20 hrs postmortem while it decreased at 8 hrs postmortem.

Shaaban *et al.*, [40] reported that there was a

[Downloaded from mail.ijrr.com on 2026-11-11]

[DOI: 10.61186/ijrr.24.4.26]

statistically significant positive (direct) correlation between the time after death (postmortem interval) and NO in both brain and liver. Also, in a study conducted by Abo El-Noor *et al.*, [41], it was found that NO was significantly increased at 4 to 5 hours in heart tissue and at 5 to 6 hours in kidney tissue after death.

Uric acid levels in the current study were determined in homogenates postmortem liver tissue and recorded a significant regular increment at (6, 8, and 20 hrs postmortem) with (0.8, 2, and 3 folds increases over normal), respectively revealed cellular nucleic material damage due to the oxidative trauma caused by high-dose irradiation.

Zhu *et al.* [36] discussed that creatinine and blood urea nitrogen showed a tendency to increase depending on the survival time, and their moderate to marked elevation accompanied by hyperuricemia, which observed in cases of delayed death, especially those with uremia, thus, confirming the usefulness of these markersfor postmortem diagnosis of renal failure, as has been reported previously. Moreover, they pointed to purineuric acid precursorsas products through the breakdown of nucleic acids in the muscle tissues and the subsequent enzymatic conversion into uric acid mainly in the liver.

Liver histopathological changes in normal death are not visible under light microscope at postmortem intervals of less than one day [42]. While in the current study, as the death was caused by supra-lethal irradiation dose liver tissue showed marked damage characterized by nuclei shrinkage, and partial hepatocytes degradation, at 6 hours after death. While after 8 hours, the nuclei completely disappeared, but at 20 hours after death, the liver cell structure itself had typically vanished. All those findings were recorded by Garczyńska *et al.* [43] in their study at 2 hrs postmortem. Their histological examination of the liver showed irregular hepatocytes borders and was loosely packed, with no visible presence of glycogen. At this point, the nuclei appeared hyperchromatic. At 10 hrs postmortem, the most prominent changes that the formerly round hepatocytes observed at 2 hrs postmortem became elongated, taking on an ellipsoidal shape; the size of hepatocytes appeared to be smaller compared to 2 hrs postmortem. Cell walls become less distinct, making it harder to visually separate hepatocytes from one another. Moreover, nuclei became smaller and exhibited signs of hyperchromasia and pyknosis.

The current study revealed that radiation exposure causes severe liver damage and portal vein area shrinkage associated with fibrillation of the vascular component as well as diffuse hemosiderosis between the hepatocytes due to the heavy burden of free radicals. These findings are in agreement with the study of Zhou *et al.* [44].

Mohammed *et al.*, [45] examined the brain post-mortem at different intervals (0, 4, 8, 12, and 24 hrs) and stated that from 0 hr to 4 hrs post-mortem, sections of cerebral cortex and cerebellum showed normal histological architectures. In contrast, our results showed the striatum of the cerebrum as well as the cerebellum showed severe congestion in the blood vessels and capillaries associated with diffuse gliosis. Moreover, they found that at 12 hrs post-mortem, there was an increase in the number of apoptotic neurons with vacuolations in the cerebral cortex, moderate apoptosis was detected in the cerebellum. In addition, at 24 hrs post-mortem, there was neuronal degeneration, vacuolations, and perivascular edema in the cerebral cortex and some necrotic cells, granular cells, and vacuolated layer in the cerebellum.

In accordance, the brain histopathological sections figure 3 showed damage due to irradiation represented by the striatum of the cerebrum and cerebellum congestion in the blood vessels and capillaries associated with diffuse gliosis as shown in histopathological examination.

Finally, the current study noticed microbial existence and its distribution in bone marrow at the different postmortem intervals, as shown in figure (1 -x & y). Microbial forensics is an effective tool in forensic investigations. Postmortem proliferation of the internal microbiome can be used to estimate the cause and the time of death [46]. These findings interpreted as a following; after death, as the intestinal barrier disappears, bacteria enter the blood stream and different organs, including the liver, pericardial fluid, and spleen, which are important for bacteriological mortality after death. Soon after death, the first region where bacteria can be found is the blood [47].

CONCLUSION

The present research is considered an addition to forensic science in terms of explaining the main cause of death as a result of exposure to supra-lethal irradiation dose. The destruction of the bone marrow and failure of its mechanism for producing immune cells (innate), leads to immune system breakdown then microbiome invasion. Subsequently, this leads to the absence of the most important means of communication between cells and cells and between cells and organs. In addition, disturbance occurred in the biochemical (function) and histological (organ barriers and cell membrane) integrity of brain and liver. Then, multi-organ failure and death arise.

***Conflict of interest*:** The authors declare that they have no competing interests

***Funding*:** This research did not receive any specific grant from any funding agencies.

***Ethics approval*:** The management of experimental animals was achieved by adhering to the rules for

[Downloaded from mail.ijrr.com on 2026-11-11]

[DOI: 10.61186/ijrr.24.4.26]

experimental research ethics approved by the Ethics Committee at NCRRT belongs to Egyptian Atomic Energy Authority. The study was conducted according to NCRRT-REC guidelines for animal painless procedures, with appropriate sedation to avoid pain and stress. Approval Number: 38A/22.

***Author contribution*:** W.T.T.: conceived and designed the study. M.R.M. and M.M.A.: analyzed the data and performed genetic studies. S.A.M. and Z.S.S.: performed biochemical studies and histopathology. All authors: Interpretation and discussion of all gained data, writing and critical review.

***AI usage*:** The authors declared that AI wasn't used for manuscript preparation.

The datasets used and/or analyzed during the current study are available from the corresponding author on reasonable request.

REFERENCES

1. International Atomic Energy Agency (2020) Medical management of radiation injuries. Safety Reports Series No. 101, IAEA, Vienna.
2. Young ST, Wells JD, Hobbs GR, Bishop CP (2013) Estimating postmortem interval using RNA degradation and morphological changes in tooth pulp. *Forensic SciInt,* ***229****(1-3): 163.e1-163.e6*.
3. Prieto-Castelló MJ, Hernández del Rincón JP, Pérez-Sirvent C, Alvarez-Jiménez P, *et al.* (2007) Application of biochemical and X-ray diffraction analyses to establish the postmortem interval. *Forensic SciInt,* ***172****: 112-118*.
4. Poloz YO and O'Day DH (2009) Determining time of death: temperature-dependent postmortem changes in calcineurin A, MARCKS, CaMKII, and protein phosphatase 2A in mouse. *Int J Legal Med,* ***123****(4): 305-314*.
5. Vrselja Z, Daniele SG, Silbereis J, *et al.* (2019) Restoration of brain circulation and cellular functions hours post-mortem. *Nature,* ***568****: 336-343*.
6. Shrestha R, Kanchan T, Krishan K (2024) Methods of estimation of time since death. In: StatPearls [Internet]. Treasure Island (FL): StatPearls Publishing; Jan 2024.
7. Zapico SC and Adserias-Garriga J (2022) Postmortem interval estimation: New approaches by the analysis of human tissues and microbial communities' changes. *Forensic Sci,* ***2****: 163-174*.
8. Da Fonseca CA, Paltian J, Dos Reis AS, Bortolatto CF, Wilhelm EA, Luchese C (2019) Na+/K+-ATPase, acetylcholinesterase and glutathione S-transferase activities as new markers of postmortem interval in Swiss mice. *Legal Med,* ***36****: 67-72*.
9. Darko M, Daniela G, Dimitrios T (2014) Nitric oxide-related oxidative stress and redox status in health and disease. *Oxid Med Cell Longev,* ***2014****: 129651*.
10. Salim S (2017) Oxidative stress and the central nervous system. *J PharmacolExpTher,* ***360****(1): 201-205*.
11. Donaldson AE and Lamont IL (2013) Biochemistry changes that occur after death: potential markers for determining post-mortem interval. *PLoS One,* ***8****(11): e82011*.
12. Kim D, Moon JS, Kim JE, *et al.* (2024) Evaluation of purine-nucleoside degrading ability and *in- vivo* uric acid lowering of Streptococcus thermophilus IDCC 2201, a novel antiuricemia strain. *PLoS One,* ***19****(2): e0293378*.
13. Ito S, Kudo K, Imamura T, *et al.* (1998) Sensitive determination of methomyl in blood using gas chromatography–mass spectrometry as its oxime tert. -butyldimethylsilyl derivative. *J Chromatogr B Biomed SciAppl,* ***713****(2): 32*.
14. Nusair SD, Mohammad Ananbeh, Zayed A, *et al.* (2022) Postmortem sampling time effect on toxicity biomarkers in rats exposed to an acute lethal methomyl dose. *Toxicol Rep,* ***9****: 1674-1680*.
15. Schmid W (1975) The micronucleus test. *Mutat Res,* ***31****: 9-15*.
16. Abdollahi, E and Mozdarani, H (2023) Role of the circ-HIPK3, circ-PVT1, miR-25, and miR-149 in response of breast cancer cells to ionizing radiation. *Cell Journal,* ***25****(10): 688-695*.
17. Banchroft JD, Layton C, Suvarna SK (2013) Bancroft's theory and practice of histological techniques. 7th ed. Churchill Livingstone, Elsevier, New York, London, San Francisco, Tokyo.
18. Mozdarani H, Mozdarani S, Pakniyat F, *et al.* (2025) Cytogenetic and cytotoxic effects of melatonin and saffron on lymphocytes of luminal A and luminal B breast cancer patients irradiated *in-vitro*. *Int J Radiat Res,* ***23****(1): 37-43*.
19. Stassi C, Mondello C, Baldino G, Ventura Spagnolo E (2020) Post-mortem investigations for the diagnosis of sepsis: a review of literature. *Diagnostics,* ***10****(10): 849*.
20. Tozzo P, Scrivano S, Sanavio M, Caenazzo L (2020) The role of DNA degradation in the estimation of post-mortem interval: a systematic review of the current literature. *Int J MolSci,* ***21****: 3540*.
21. Huang W, Zhao S, Liu H, Pan M, Dong H (2024) The role of protein degradation in estimation postmortem interval and confirmation of cause of death in forensic pathology: a literature review. *Int J MolSci,* ***25****(3): 1659*.
22. Kotenko KV, Kvacheva YE, Granovskaya EO, Kukhta BA (2015) Forensic and medical aspects of radiation accidents investigation. In: Advances in nuclear forensics: countering the evolving threat of nuclear and other radioactive material out of regulatory control. Proceedings of an International Conference. Companion CD-ROM.
23. Berger ME, O'Hare FM Jr, Ricks RC, eds. (2002) The medical basis for radiation accident preparedness: the clinical care of victims. REAC/TS Conference on the Medical Basis for Radiation Accident Preparedness. New York: Parthenon Publishing.
24. Malara A, Abbonante V, Di Buduo CA, *et al.* (2015) The secret life of a megakaryocyte: emerging roles in bone marrow homeostasis control. *Cell Mol Life Sci,* ***72****(8): 1517-1536*.
25. Michalova J, Savvulidi F, Sefc L, *et al.* (2011) Cadaveric bone marrow as potential source of hematopoietic stem cells for transplantation. *Chimerism,* ***2****(3): 86-87*.
26. Murakami S, Yoshino H, Ishikawa J, *et al.* (2015) Effects of ionizing radiation on differentiation of murine bone marrow cells into mast cells. *J Radiat Res,* ***56****(6): 865-871*.
27. Suchacki KJ, Tavares AAS, Mattiucci D, *et al.* (2020) Bone marrow adipose tissue is a unique adipose subtype with distinct roles in glucose homeostasis. *Nat Commun,* ***11****: 3097*.
28. Li Z, Bowers E, Zhu J, *et al.* (2022) Lipolysis of bone marrow adipocytes is required to fuel bone and the marrow niche during energy deficits. *eLife,* ***11****: e78496*.
29. Krebsbach PH, Kuznetsov SA, Bianco P, Robey PG (1999) Bone marrow stromal cells: characterization and clinical application. *Crit Rev Oral Biol Med,* ***10****(2): 165-181*.
30. Sakr MF, El-Khalek AMA, Mohammad NS, *et al.* (2023) Estimation of postmortem interval using histological and oxidative biomarkers in human bone marrow. Forensic Sci Med Pathol.
31. Gururaj B, Kumar GP, Shaila B, Nayak VC (2015) Correlation of cellular autolytic changes in bone marrow with post-mortem interval. *Int. J Clinical and Biomedical Research,* ***1****(4): 28-33*.
32. Satish Babu BS, Biradar G, Bakkannavar S, *et al.* (2015) Estimation of time since death from nuclei changes of bone marrow cells. *Indian J Forensic Community Med,* ***2****(4): 198-202*.
33. Findlay AB (1977) Bone marrow changes in the postmortem interval. J Forensic *SciSoc,* ***16****: 213-218*.
34. Kvacheva YE (2000) Human bone marrow repair processes and cell populations in acute radiation injury: a morphological study. *Radiat Biol Radioecol,* ***40****(1): 5-9*.
35. Suzuki K, Imaoka T, Tomita M, *et al.* (2023) Molecular and cellular basis of the dose-rate-dependent adverse effects of radiation exposure in animal models. Part II: hematopoietic system, lung and liver. *J Radiat Res,* ***64****(2): 228-249*.
36. Zhu BL, Ishikawa T, Michiue T, *et al.* (2007) Differences in postmortem urea nitrogen, creatinine and uric acid levels between blood and pericardial fluid in acute death. *Legal Med,* ***9****(3): 115-122*.
37. McHardy SF, Wang HL, McCowen SV, Valdez MC (2017) Recent advances in acetylcholinesterase inhibitors and reactivators: an update on the patent literature (2012–2015). *Expert Opin Ther Pat,* ***27****(4): 455-476*.
38. Krassner MM, Kauffman J, Sowa A, *et al.* (2023) Postmortem changes in brain cell structure: a review. *Free Neuropathol,* ***4****: 4-10*.
39. Yao LH, Jiang YM, Shi J, *et al.* (2004) Flavonoids in food and their health benefits. *Plant Foods Hum Nutr,* ***59****(3): 113–122*.
40. Shaaban DAAER, Farrag DIM, Bayoumy A, Saad E (2017) Estimation of early postmortem interval by biochemical changes in brain and liver of rats using some oxidant and antioxidant parameters. *Egypt J Forensic SciApplToxicol,* ***17****(1): 147-162*.
41. Abo El-Noor MM, Elhosary NM, Khedr NF, El-Desouky KI (2016) Estimation of early postmortem interval through biochemical and pathological changes in rat heart and kidney. *Am J Forensic Med*

[Downloaded from mail.ijrr.com on 2026-11-11]

[DOI: 10.61186/ijrr.24.4.26]

Pathol, ***37****(1): 40-46*.
42. Ceciliason AS, Andersson MG, Nyberg S, Sandler H (2021) Histological quantification of decomposed human livers: a potential aid for estimation of the post-mortem interval? *Int J Legal Med,* ***135****(1): 253-267*.
43. Garczyńska K, Tzschätzsch H, Assili S, *et al.* (2021) Effect of post-mortem interval and perfusion on the biophysical properties of ex vivo liver tissue investigated longitudinally by MRE and DWI. *Front Physiol,* ***12****: 696304*.
44. Zhou YJ, Tang Y, Liu SJ, *et al.* (2023) Radiation-induced liver disease: beyond DNA damage. *Cell Cycle,* ***22****(5): 506-526*.
45. Mohammed AT, Abdelfattah-Hassan A, Abdo S, *et al.* (2023) Estimation of the time since death based on the post-mortem histopathological changes in a rat brain: an observational study. *J Adv Vet Res,* ***13****(3): 526-530*.
46. Yousef Saber F, Naseri Z, Hasani AH (2022) A short review of forensic microbiology. *Avicenna J ClinMicrobiol Infect,* ***9****(2): 88-96*.
47. Adserias-Garriga J, Quijada NM, Hernandez M, *et al.* (2017) Dynamics of the oral microbiota as a tool to estimate time since death. *Mol Oral Microbiol,* ***32****: 511-516*.

[Downloaded from mail.ijrr.com on 2026-11-11]

[DOI: 10.61186/ijrr.24.4.26]

[DOI: 10.61186/ijrr.24.4.26] [Downloaded from mail.ijrr.com on 2026-11-11]